Enhancement and suppression of spatial splitting four-wave mixing in atomic medium*

Zhuang Yu-Ming(庄雨茗)[a], Sang Su-Ling(桑苏玲)[a)b)], Li Pei-Ying(李培英)[a)], Yuan Chen-Zhi(袁晨智)[a)], Huo Shu-Li(霍淑利)[a)], Xue Xin-Xin(薛鑫鑫)[a)], Wang Zhi-Guo(王志国)[a)], Zheng Huai-Bin(郑淮斌)[a)], and Zhang Yan-Peng(张彦鹏)[a)†]

[a)] *Key Laboratory for Physical Electronics and Devices of the Ministry of Education & Shaanxi Key Laboratory of Information Photonic Technique, Xi'an Jiaotong University, Xi'an* 710049, *China*

[b)] *School of Physics and Information Technology, Ningxia Teachers University, Guyuan* 756000, *China*

(Received 22 July 2011; revised manuscript received 19 August 2011)

We experimentally report on the evolution from singly-dressed to doubly-dressed four-wave mixing (FWM) process by controlling the powers of the probe, the pump and the dressing fields respectively. The differences in the enhancement and the suppression of FWM signal between the two-level and cascade three-level atomic systems are observed and explained by the multi-dressed effect theoretically. Both the x direction and the y direction spatial splittings of the degenerate-FWM (DWFM) beams are obtained. We also investigate the switch between the enhancement and the suppression of the DWFM signals and between its spatial splittings in x direction and y direction. The spatial splittings in x direction and y direction can be controlled by the relative position and the intensity of the involved laser beams. Such a study can be useful for optimizing the efficiency of the FWM process and providing potential applications in spatial signal processing.

Keywords: four-wave mixing, spatial splitting, enhancement, suppression

PACS: 42.50.Gy **DOI:** 10.1088/1674-1056/21/2/024204

1. Introduction

The spatial focusing of one weak laser beam by another stronger beam in Kerr nonlinear optical medium has been demonstrated.[1−5] Such a spatial modulation effect is governed by the cross-phase modulation (XPM) between the two laser beams in Kerr nonlinear medium.[4−6] Also, the efficient four-wave mixing (FWM) processes enhanced by atomic coherence in multilevel atomic systems has been investigated and demonstrated in previous research.[7−13] The crucial elements of such enhanced nonlinear optical processes lie in the enhanced nonlinear susceptibility because of the induced atomic coherence as well as greatly reduced linear absorption of the generated optical field due to electromagnetically induced transparency. The XPM as well as the modified self-phase modulation can significantly affect the propagations and the spatial patterns of the traveling laser beams when several laser beams propagate through an atomic medium.[1−3] Recently, our work involved the investigation of the doubly dressed schemes in a five-level atomic system[12] and the observation of the three-peak Autler–Townes splitting of doubly-dressed FWM signal.[13]

In the present paper, we first investigate the connection between the switch signal and the spatial splitting of the degenerate-FWM (DWFM), from the pure-enhancement to first suppression and then enhancement. By carefully controlling the powers of the probe and the dressing fields, the DWFM signal can be switched easily. The enhancement and the suppression of the DWFM signals between two-level atomic system and cascade three-level atomic system are compared. Then we show the evolution of the FWM process from singly-dressed to doubly-dressed by controlling the power of the pump fields. In addition, the simultaneously observed spatial splittings of the DWFM signal in the x direction and the y direction are analysed. Such a study opens doors for

*Project supported by the 973 Program of China (Grant No. 2012CB921804), the National Natural Science Foundation of China (Grant Nos. 10974151, 61078002, 61078020, 11104214, 61108017, and 11104216), the New Century Excellent Talent Project of the Ministry of Education of China (Grant No. 08-0431), and the Interdisciplinary Project of Xi'an Jiaotong University, China (Grant Nos. xjj20100100 and xjj20100151).

†Corresponding author. E-mail: ypzhang@mail.xjtu.edu.cn

© 2012 Chinese Physical Society and IOP Publishing Ltd

future spatial signal processing, the optical communication and the optimization of the efficiencies of the FWM processes.

2. Basic theory

The experiment is conducted in sodium atoms (in a heat pipe oven) involving a cascade three-level atomic system and a two-level atomic system as shown in Fig. 1(a). In the two-level atomic system (the left part in Fig. 1(a)) composed of the energy levels $|0\rangle$ ($3S_{1/2}$) and $|1\rangle$ ($3P_{3/2}$), the pump laser fields $\boldsymbol{E}_1$ (with frequency ω_1, wave vector $\boldsymbol{k}_1$, and the Rabi frequency G_1) and $\boldsymbol{E}_1'$ (ω_1, $\boldsymbol{k}_1'$, and G_1') propagate in the opposite directions and $\boldsymbol{E}_1'$ propagates in the direction opposite to the direction of the probe field $\boldsymbol{E}_3$ (ω_1, $\boldsymbol{k}_3$, and G_3), with a small angle ($\sim 0.3^\circ$) included between them. These three beams are from the same near-transform-limited dye laser (with a 10-Hz repetition rate, 5-ns pulse width and 0.04-m^{-1} linewidth) with the same frequency detuning $\Delta_1 = \Omega_{10} - \omega_1$, where Ω_{10} is the transition frequency between $|0\rangle$ and $|1\rangle$. The dressing field E_2 (ω_2, k_2, G_2) is from another near-transform-limited dye laser with the frequency detuning $\Delta_2 = \Omega_{10} - \omega_2$, where Ω_{21} is the transition frequency between $|0\rangle$ and $|1\rangle$, and it propagates collinearly with E_1. When E_2 is blocked, a degenerate-FWM (DFWM) ($E_{\rm F1}$) process (Fig. 1(a)) satisfying the phase-matching condition $\boldsymbol{k}_{\rm F1} = \boldsymbol{k}_1 - \boldsymbol{k}_1' + \boldsymbol{k}_3$ is obtained. With four laser beams on, the dressed DFWM process is generated. In the cascade three-level atomic energy, the experimental scheme is similar. The pulse laser beams are spatially aligned as shown in Figs. 1(b) and 1(c), with energy level $|0\rangle$ ($3S_{1/2}$), $|1\rangle$ ($3P_{1/2}$), $|2\rangle$ ($3P_{3/2}$) as shown in Fig. 1(a). The difference is that field $\boldsymbol{E}_2$ (ω_2, $\boldsymbol{k}_2$, G_2) is connected to the transition between $|1\rangle$ and $|2\rangle$, with the detuning frequency $\Delta_2 = \Omega_{21} - \omega_2$, where Ω_{21} is the transition frequency between $|1\rangle$ and $|2\rangle$, while a similar result can be obtained when $\boldsymbol{E}_2$ is on or blocked. The spatial splitting images of the generated DFWM signal are captured by a CCD camera and by discretely choosing different values of detuning Δ_1 (with different powers of the pump field, probe field and dressing field) and scanning Δ_2, its enhancement/suppression can be recorded by PMT.

In order to model the four-wave mixing process, the perturbation chain (Liouville pathway) is introduced. First, in the two-level atomic system, considering $\boldsymbol{E}_{\rm F1}$ dressed by $\boldsymbol{E}_1$ ($\boldsymbol{E}_1'$) and $\boldsymbol{E}_2$, the Liouville pathway of the multi-dressed DFWM $\rho_{00}^{(0)} \xrightarrow{(E_1)*} \rho_{(G_1G_2\pm)(G_1G_2\pm)}^{(1)} \xrightarrow{(E_1')*} \rho_{00}^{(2)} \xrightarrow{E_3} \rho_{(G_1G_2\pm)(G_1G_2\pm)}^{(3)}$, and therefore the third-order density matrix element, of which the module determines the intensity of DFWM, can be expressed as

$$\begin{aligned}\rho_{10}^{(3)} = & -\mathrm{i}\, G_3 G_1 (G')_1^* / (d_1 + |G_1|^2/\Gamma_{00} \\ & + |G_1|^2/\Gamma_{11} + |G_2|^2/d_3 \\ & + |G_2|^2/d_4)^2 (\Gamma_{00} + |G_1|^2/d_1 + |G_1|^2/d_2 \\ & + |G_2|^2/d_5 + |G_2|^2/d_6),\end{aligned}$$

where $d_1 = \Gamma_{10} + \mathrm{i}\,\Delta_1$, $d_2 = \Gamma_{01} - \mathrm{i}\,\Delta_1$, $d_3 = \Gamma_{00} + \mathrm{i}(\Delta_1 - \Delta_2)$, $d_4 = \Gamma_{11} + \mathrm{i}(\Delta_1 - \Delta_2)$, $d_5 = \Gamma_{10} + \mathrm{i}\,\Delta_2$, and $d_6 = \Gamma_{01} - \mathrm{i}\,\Delta_2$, with Γ_{ij} being the transverse relaxation rate between the states $|i\rangle$ and $|j\rangle$ (the term has been introduced). Similarly, in the cascade three-level system, when $\boldsymbol{E}_{\rm F1}$ is also dressed by the fields $\boldsymbol{E}_1$ and $\boldsymbol{E}_2$, the multi-dressed Liouville pathway in such a case is $\rho_{00}^{(0)} \xrightarrow{(E_1)*} \rho_{G_1\pm G_2\pm G3}^{(1)} \xrightarrow{(E_1')*} \rho_{00}^{(2)} \xrightarrow{E_3} \rho_{G_1\pm G_2\pm G3}^{(3)}$, we can obtain

$$\begin{aligned}\rho_{10}^{(3)} = & -\mathrm{i}\, G_3 G_1 (G_1')^* / [(d_1 + |G_1|^2/\Gamma_{00} \\ & + |G_1|^2/(\Gamma_{00} + A) + |G_3|^2/\Gamma_{00} \\ & + |G_3|^2/(\Gamma_{11} + A) + |G_2|^2/d_7]^2 [\Gamma_{00} \\ & + |G_1|^2/(d_1 + A_2) + |G_1|^2/(d_2 + A_3) \\ & + |G_3|^2/(d_1 + A_2) + |G_3|^2/(d_2 + A_3)],\end{aligned}$$

where $d_7 = \Gamma_{20} + \mathrm{i}(\Delta_1 + \Delta_2)$, $A_1 = |G_2|^2/(\Gamma_{21} + \mathrm{i}\,\Delta_2)$,

$$A_2 = |G_2|^2/[\Gamma_{20} + \mathrm{i}(\Delta_1 + \Delta_2)],$$

and

$$A_3 = |G_2|^2/[\Gamma_{02} - \mathrm{i}(\Delta_1 + \Delta_2)].$$

In addition, the Doppler effect and the power broadening effect on the weak FWM signals need to be considered.

To model the spatial effects of the DFWM signal in propagation, we need to consider the XPM enhanced by the dressing effects. In both the two atomic systems mentioned above, the spatial modulation of the DFWM signal is caused mainly by the nonlinear cross-Kerr effect of $\boldsymbol{E}_1'$, and the electromagnetically induced grating (EIG) is induced by the interference between the beams $\boldsymbol{E}_1$ and $\boldsymbol{E}_1'$.[3] On the one hand, the nonlinear phase shift introduced by the XPM is $\phi = 2\boldsymbol{k}_{\rm F1} n_2 z I_1\, \mathrm{e}^{-r^2/2}/(n_0 I_{\rm F1}')$, where n_2 is the nonlinear cross-Kerr refractive index; I_1 is the intensity of the laser beam $\boldsymbol{E}_1'$; $I_{\rm F1}'$ is the intensity of $\boldsymbol{E}_{\rm F1}$. On the other hand, the beams $\boldsymbol{E}_1$ and $\boldsymbol{E}_1'$ are aligned in the y–z plane with an angle $\theta = 0.05^\circ$ to induce the grating with the fringe spacing $\Lambda = \lambda_1/\theta$.

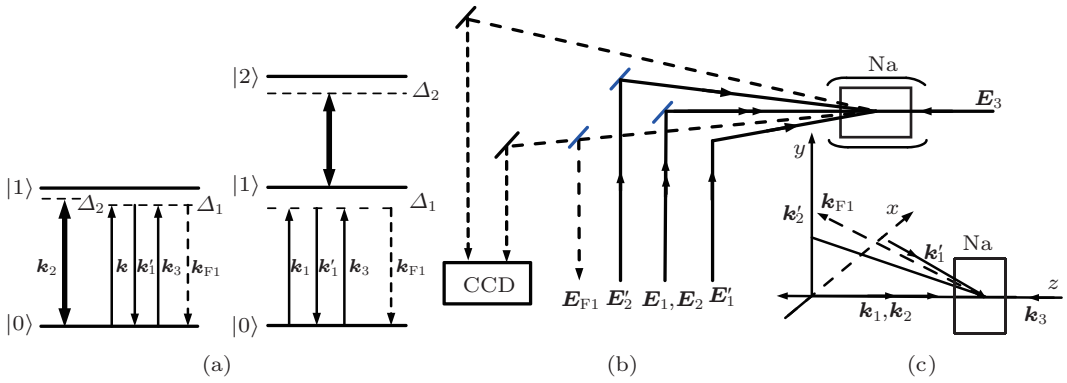


Fig. 1. (colour online) (a) Diagrams of the two-level atomic system and the cascade three-level atomic system, (b) spatial beam geometry of the experiment and (c) spatial alignments of the incident beams.

3. Experiment result analysis

When the four laser beams: strong dressing field $\boldsymbol{E}_2$ and weak fields $\boldsymbol{E}_1$, $\boldsymbol{E}_1'$, and $\boldsymbol{E}_3$, are all on, the suppression and the enhancement of the singly-dressing $\boldsymbol{E}_{\rm F1}$ in both the cascade three-level and two-level systems are shown in Fig. 2(a). In both systems, when Δ_1 is scanned, a global single peak can be observed as shown in Figs. 2(a1) and 2(a2). Then we set Δ_1 to be at different discrete points from the negative to positive region and scan Δ_2 near the transition centre, the intensity of $\boldsymbol{E}_{\rm F1}$ evolves from pure-enhancement to first suppression and then enhancement, to pure-suppression, to first enhancement and then suppression, to pure-enhancement sequentially as shown in Fig. 2(a1) in two-level system. While in cascade three-level system, the intensity of $\boldsymbol{E}_{\rm F1}$ evolves from pure-enhancement to first enhancement and then suppression, then to pure-suppression, further to first suppression and then enhancement and finally to pure-enhancement (Fig. 2(a2)).

To better explain the results mentioned above, the different characteristics of the two atomic systems are investigated. The Liouville pathway for the pure DFWM in both systems is $\rho_{00}^{(0)} \xrightarrow{(\boldsymbol{E}_1)*} \rho_{10}^{(1)} \xrightarrow{(\boldsymbol{E}_1')*} \rho_{00}^{(2)} \xrightarrow{\boldsymbol{E}_3} \rho_{10}^{(3)}$, and the corresponding third-order nonlinear susceptibility is $\rho_{10}^{(3)} = -\mathrm{i}\,G_3G_1(G')_1^*/(d_1^2\Gamma_{00})$. Therefore, when Δ_1 is scanned from the negative to the positive region (Figs. 2(c1)–2(d1)) at $G_2 = 0$, the intensity of $\boldsymbol{E}_{\rm F1}$ is strongest at $\Delta_1 = 0$ as shown in Figs. 2(a) and 2(b). In both systems, the dressing field $\boldsymbol{E}_2$ will split the energy level $|1\rangle$ into two dressed states $|G_2\pm\rangle$ (Figs. 2(c) and 2(d)). Under this singly-dressing condition, the Liouville pathway in the two-level system is modified into $\rho_{00}^{(0)} \xrightarrow{(\boldsymbol{E}_1)*} \rho_{G_2\pm0}^{(1)} \xrightarrow{(\boldsymbol{E}_1')*} \rho_{00}^{(2)} \xrightarrow{\boldsymbol{E}_3} \rho_{G_2\pm0}^{(3)}$, and the third-order nonlinear susceptibility into $\rho_{10}^{(3)} = -\mathrm{i}\,G_3G_1(G')_1^*/[(d_1 + |G_2|^2/d_3)^2\Gamma_{00}]$, while in cascade three-level system, the singly-dressed perturbation chain stays the same as that in the two-level system, but it leads to a different susceptibility $\rho_{10}^{(3)} = -\mathrm{i}\,G_3G_1(G')_1^*/[(d_1 + |G_2|^2/d_7)^2\Gamma_{00}]$. In the two-level system, when Δ_2 is scanned and the probe field is set to be far away from the resonance point at $\Delta_1 < 0$, the pure-enhancement is acquired as shown in curve 1 of Fig. 2(a1) because the probe field $\boldsymbol{E}_3$ gradually approaches to the dressed state $|G_2+\rangle$ to satisfy the enhancement condition $\Delta_1 - \Delta_2 + G_2 = 0$ (Fig. 2(c2)).[7] Similar results can be seen from curve 1 of Fig. 2(a2) in the cascade three-level system because the enhancement condition $\Delta_1 + \Delta_2 + G_2 = 0$ is satisfied. When Δ_2 is scanned while the probe field is near the resonance point at $\Delta_1 < 0$ in the two-level system, $\boldsymbol{E}_{\rm F1}$ is first suppressed and then enhanced (curve 2 of Fig. 2(a1)) because the suppression condition $\Delta_1 - \Delta_2 = 0$ is first satisfied due to two-photon resonance (Fig. 2(c3)) and the enhancement condition $\Delta_1 - \Delta_2 + G_2 = 0$ is then matched due to the resonance to the dressed state $|G_2+\rangle$ (Fig. 2(c4)). However, in the cascade three-level system, $\boldsymbol{E}_{\rm F1}$ is first enhanced and then suppressed as shown in curve 2 of Fig. 2(a2) because the order of the successive resonances is just opposite to that in the two-level system. For the point $\Delta_1 = 0$, $\boldsymbol{E}_{\rm F1}$ is suppressed in both systems as shown in curve 3 of Figs. 2(a1) and 2(a2), because the suppression conditions $\Delta_1 - \Delta_2 = 0$ in the two-level system and $\Delta_1 + \Delta_2 = 0$ in the cascade three-level system are satisfied, respectively. When Δ_2 is scanned at $\Delta_1 > 0$, there exist evolutions of the DFWM signal symmetrical to those in the region with $\Delta_1 > 0$, as shown in Figs. 2(c5)–2(c8). The experimental results accord well with the theoretical results.

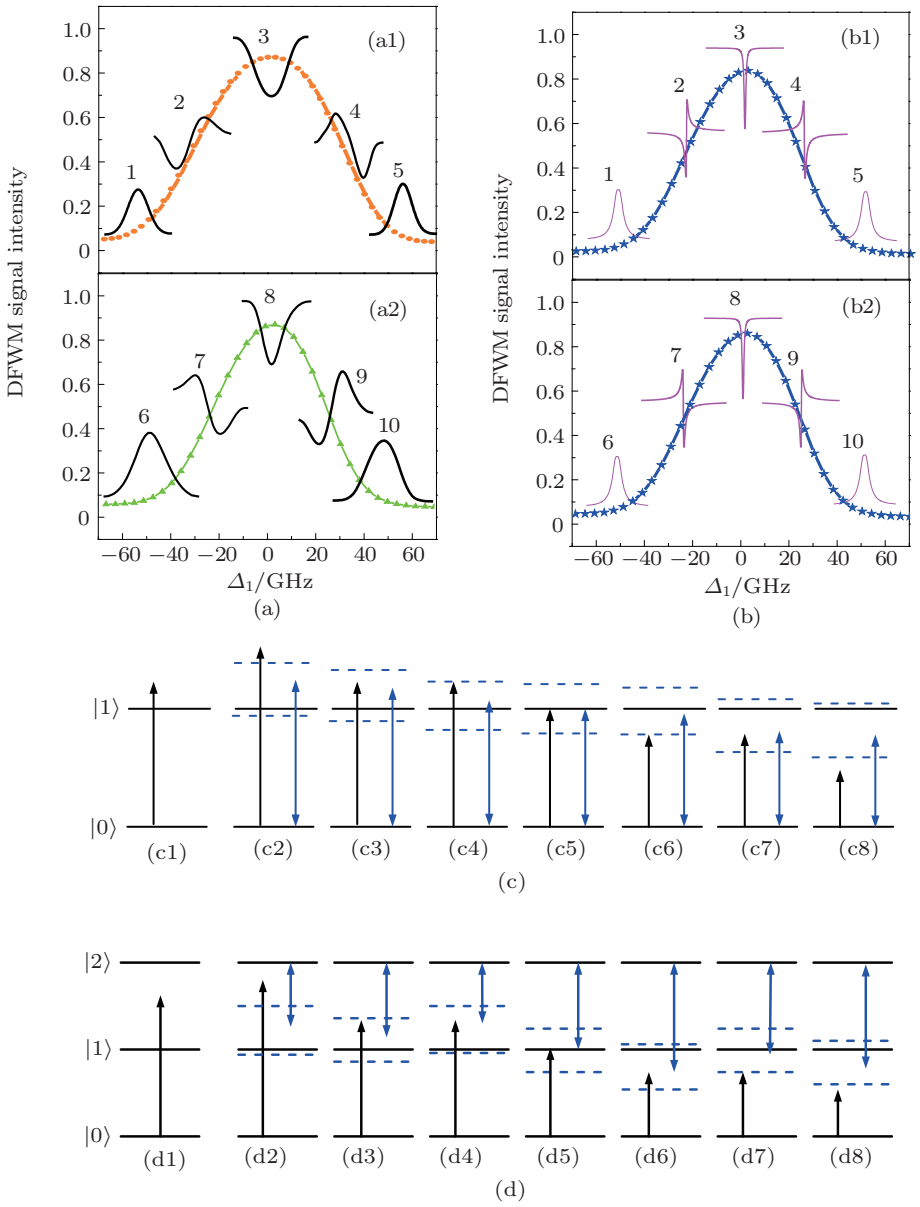


Fig. 2. (colour online) (a) Experimental results of the singly-dressed $\boldsymbol{E}_{\rm F1}$ at $P_1 = 10$ μW, $P_2 = 25$ μW, $P_3 = 10$ μW in (a1) two-level system and (a2) cascade three-level system when $\boldsymbol{E}_2'$ is blocked. Measured suppressed and enhanced DFWM signals versus Δ_2 at different Δ_1 values: $\Delta_1 = -53.4$ (curve 1), –30.5 (curve 2), 0 (curve 3), 31.2 (curve 4), 55.7 (curve 5), –50.2 (curve 6), –28.7 (curve 7), 0 (curve 8), 29.5 (curve 9), 50.1 (curve 10) GHz; (b) Theoretical results of the singly-dressed $\boldsymbol{E}_{\rm F1}$ in both cascade three-level system and two-level system. The conditions are the same as those in Fig. 2(a); (c) The dressed-state pictures of the suppression or enhancement of the $\boldsymbol{E}_{\rm F1}$ in two-level system. The dressed states $|G_2\pm\rangle$ are denoted with dashed lines; (d) The dressed-state pictures of the suppression or enhancement of $\boldsymbol{E}_{\rm F1}$ in cascade three-level system. The dressed states $|G_2\pm\rangle$ are denoted with dashed lines.

Next, when $\boldsymbol{E}_2$ and $\boldsymbol{E}_1(\boldsymbol{E}_1')$ are both sufficiently strong, the suppression and the enhancement of the doubly-dressed $\boldsymbol{E}_{\rm F1}$ accompanied by its spatial splitting in the y direction can be observed in Figs. 3(a) and 3(b). Here Figs. 3(a1)–3(a4) showing the splitting of $\boldsymbol{E}_{\rm F1}$ signal correspond to the curves in Figs. 3(b6)–3(b9).

To completely explain the splitting in the y direction of $\boldsymbol{E}_{\rm F1}$, the relative positions of various beams must be considered. In the experiment, the pump beams $\boldsymbol{E}_1$ and $\boldsymbol{E}_1'$ are deliberately aligned in the y–z plane, with a small angle θ ($\theta = 0.05°$) included between them. According to the phase matching condition, the generated $\boldsymbol{E}_{\rm F1}$ will overlap with $\boldsymbol{E}_1'$ in both x direction and y direction. But when $\boldsymbol{E}_1$ and $\boldsymbol{E}_1'$ are set to be in the middle of the heat-pipe oven, $\boldsymbol{E}_{\rm F1}$ will exactly overlap with $\boldsymbol{E}_1'$ only in the y direction. Furthermore, because of the rather small angle θ, the

spacing of the fringes of $\boldsymbol{E}_{\rm F1}$ introduced by the modulation of EIG induced by $\boldsymbol{E}_1$ and $\boldsymbol{E}_1'$ in y–z plane, $\Lambda = \lambda_1/\theta$, is large enough to be observed. So the splitting in the y direction due to the grating is obtained as shown in Fig. 3(a). In addition, when the intensity of $\boldsymbol{E}_{\rm F1}$ is enhanced, more splitting parts are observed because of the larger spot passing through the grating. Similarly, when the intensity of $\boldsymbol{E}_{\rm F1}$ is suppressed, the splitting becomes weaker.

Figure 3(b) displays the enhancement and the suppression of the doubly-dressed $\boldsymbol{E}_{\rm F1}$. The global double-peak is obtained by scanning Δ_1 when $\boldsymbol{E}_2$ is blocked as shown in Fig. 3(b). By choosing Δ_1 directly within $\Delta_1 < 0$ and scanning Δ_2, the intensity of the DFWM signal $\boldsymbol{E}_{\rm F1}$ evolves from pure-enhancement, to first enhancement and then suppression, to pure-suppression, to first suppression and then enhancement and to pure-enhancement successively, which is clearly demonstrated on the left side of Fig. 3(b). When Δ_1 is set to be in the positive region, symmetric processes can be observed from the six curves on the right side of Fig. 3(b).

In order to explain such evolving enhancement and suppression in the doubly-dressing system, the dressed-state pictures are adopted theoretically. When the power of $\boldsymbol{E}_1$ ($\boldsymbol{E}_1'$) increases, it acts as not only the pump field but also the inner dressing field. In the cascade doubly-dressed system by $\boldsymbol{E}_1$ ($\boldsymbol{E}_1'$) and $\boldsymbol{E}_2$, the dressed Liouville pathway is $\rho_{00}^{(0)} \xrightarrow{(\boldsymbol{E}_1)*} \rho_{G_1\pm G_2\pm 0}^{(1)} \xrightarrow{(\boldsymbol{E}_1')*} \rho_{00}^{(2)} \xrightarrow{\boldsymbol{E}_3} \rho_{G_1\pm G_2\pm 0}^{(3)}$. Then we can obtain the expressions of the corresponding density matrix elements as follows: $\rho_{10}^{(3)} = -\mathrm{i}\,G_3G_1(G_1')^*/[(d_1+|G_2|^2/d_7+|G_1|^2/\Gamma_{00})^2\Gamma_{00}]$. Initially, the state $|1\rangle$ will be split into two dressed states $|G_1\pm\rangle$ by $\boldsymbol{E}_1$ ($\boldsymbol{E}_1'$) (Fig. 3(c1)). When $\boldsymbol{E}_2$ is blocked and Δ_1 is scanned, $\boldsymbol{E}_3$ can resonate with the two dressed states $|G_1\pm\rangle$ respectively to enhance the intensity of $\boldsymbol{E}_{\rm F1}$ as shown in Fig. 3(c1). So the two peaks are obtained globally as shown in Fig. 3(b).

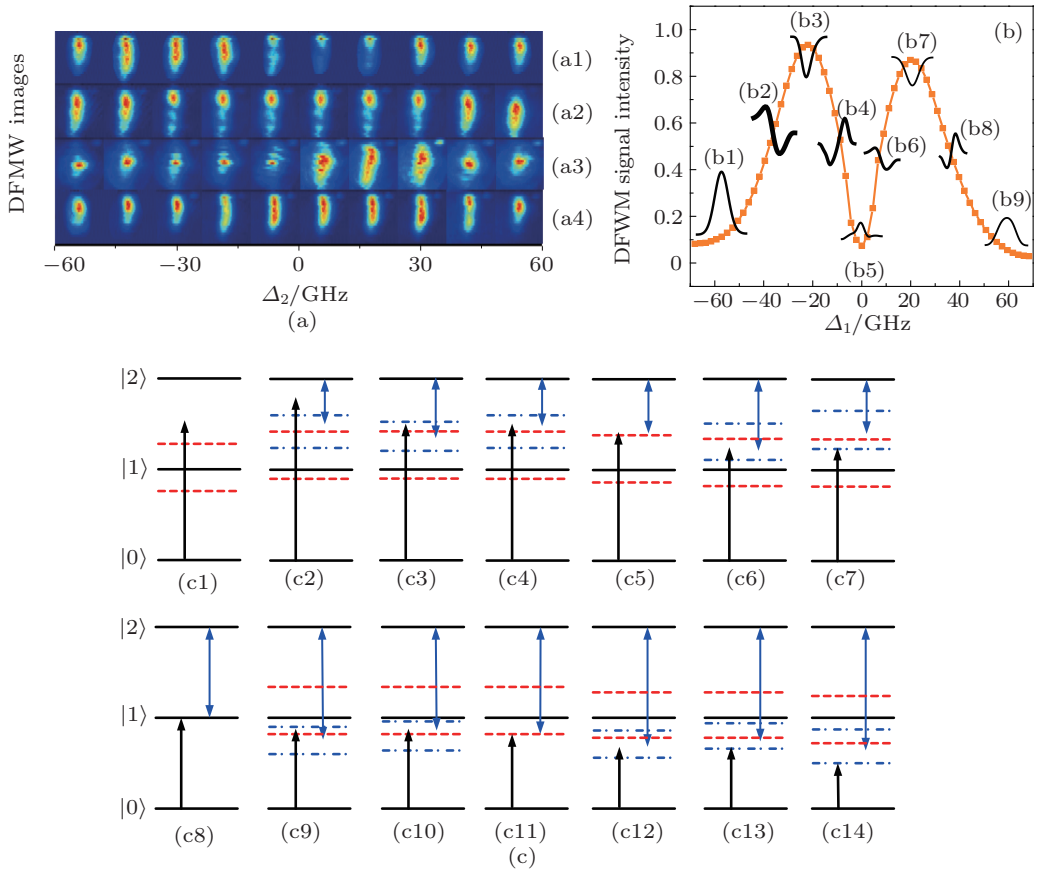


Fig. 3. (colour online) (a) $\boldsymbol{E}_{\rm F1}$ images at $\rm P_1 = 25\ \mu W$, $\rm P_2 = 28\ \mu W$, $\rm P_3 = 12\ \mu W$ when $\Delta_1 = 18.6$ (a1), 31.3 (a2), 47.9 (a3), 69.5 (a4), with $\boldsymbol{E}_2'$ blocked in the experiment; (b) experimental results of the doubly-dressed $\boldsymbol{E}_{\rm F1}$ by the dressing fields and the pump fields when $\Delta_1 = -68.5$ (b1), -48.1 (b2), -32.4 (b3), -19.8 (b4), 0 (b5), 18.6 (b6), 31.3 (b7), 47.9 (b8), 69.5 (b9) GHz, with other conditions remaining the same as those in Fig. 3(a), where the dot-dashed line represents the double-peak $\boldsymbol{E}_{\rm F1}$ versus Δ_1; (c) dressed-state pictures of the suppression or the enhancement of the $\boldsymbol{E}_{\rm F1}$, with the states $|G_1\pm\rangle$ denoted with dashed lines and the states $|G_1+G_2\pm\rangle$ or $|G_1-G_2\pm\rangle$ represented by dot-dashed lines.

Afterwards, when $\boldsymbol{E}_2$ is on, the dressed state $|G_1\pm\rangle$ is further split into the dressed states $|G_1 + G_2\pm\rangle$ or $|G_1 - G_2\pm\rangle$ by $\boldsymbol{E}_2$ (Figs. 3(c2)–3(c14)). In the region with $\Delta_1 > 0$, when Δ_2 is scanned, the intensity of $\boldsymbol{E}_{\rm F1}$ evolves from strong to weak (Fig. 3(a1)). The DWFM signal is first enhanced and then suppressed shown as in Fig. 3(b6) because $\boldsymbol{E}_3$ first resonates to the dressed state $|G_1 - G_2+\rangle$ to satisfy the enhancement condition $\Delta_1 + \Delta_2 + G_2 = 0$ and then the suppression condition $\Delta_1+\Delta_2 = 0$ is matched due to the two-photon resonance as shown in Figs. 3(c9) and 3(c10). When Δ_1 increases, $\boldsymbol{E}_{\rm F1}$ is purely suppressed as shown in Figs. 3(a2) and 3(b7) since $\boldsymbol{E}_3$ could not reach state $|G_1 - G_2\pm\rangle$ and the suppression condition $\Delta_1 + \Delta_2 = 0$ is satisfied (Fig. 3(c11)). With the value of Δ_1 further increasing, the intensity of $\boldsymbol{E}_{\rm F1}$ is first suppressed due to resonance and then enhanced due to being resonant with the dressed state $|G_1 - G_2-\rangle$ (Figs. 3(a3) and 3(b8)). When the positive Δ_1 is set to be far away from the resonance point at $\Delta_1 > 0$, the intensity of $\boldsymbol{E}_{\rm F1}$ is enhanced and therefore gradually stronger as shown in Figs. 3(a4) and 3(b9). So the pure-enhancement is acquired because $\boldsymbol{E}_3$ gradually approaches to the dressed state $|G_1 - G_2-\rangle$ (Fig. 3(c14)) and the enhancement condition $\Delta_1 + \Delta_2 - G_2 = 0$ is satisfied. At the point with $\Delta_1 = 0$, the pure-enhancement (Fig. 3(b5)) is obtained because $\boldsymbol{E}_3$ and dressing fields both reach the resonance point, satisfying the enhancement condition $\Delta_1 + \Delta_2 + G_2 = 0$ (Fig. 3(c6)). When scanning Δ_2 with $\Delta_1 < 0$ (Figs. 3(b1)–3(b4)), the intensity of $\boldsymbol{E}_{\rm F1}$ displays symmetry process and the corresponding theoretical explanations are similar. The experimental results fit well to the theoretical results.

Finally, we investigate the switch between the enhancement and the suppression of $\boldsymbol{E}_{\rm F1}$ (Fig. 4). With the powers of $\boldsymbol{E}_3$ and $\boldsymbol{E}_2$ increasing, $\boldsymbol{E}_{\rm F1}$ evolves from pure-enhancement to first suppression and then enhancement.

Figure 4(b) shows the corresponding $\boldsymbol{E}_{\rm F1}$ images in Fig. 4(a), which shows the splitting in the x direction. It is worth noting that the spatial splitting images have a transformation from the ones in x direction in Fig. 3(a) to the ones in y direction in Fig. 4(b). The x direction spatial splitting is obtained when $\boldsymbol{E}_1$ and $\boldsymbol{E}_1'$ are set to be in the front and at the back of the heat-pipe oven compared with the y direction splitting when $\boldsymbol{E}_1$ and $\boldsymbol{E}_1'$ are set to be in middle of the heat-pipe oven. Compared with the angle (0.3°) in x–z plane between $\boldsymbol{E}_1$ and $\boldsymbol{E}_1'$, the angle ($\theta = 0.05°$) in y–z plane is small enough to be ignored when they are set to be in the front or at the back of the heat-pipe oven. Furthermore, the splitting induced by the grating in x–z plane created by $\boldsymbol{E}_1$ and $\boldsymbol{E}_1'$ is too small to be observed. So the x direction splitting is obtained due mainly to the nonlinear cross-Kerr effect of $\boldsymbol{E}_1'$. In the expression of the nonlinear phase shift $\phi = 2k_{\rm F1}n_2zI_1\,{\rm e}^{-r^2/2}/(n_0I_{\rm F1}')$, ϕ is directly proportional to n_2 and I_1, but inversely proportional to $I_{\rm F1}'$. When Δ_2 is scanned, the intensity I_1 of the laser beam $\boldsymbol{E}_1'$ and the nonlinear index n_2 remain nearly constant, thus ϕ is determined mainly by $I_{\rm F1}'$. As the intensity of $\boldsymbol{E}_3$ increases, $I_{\rm F1}'$ becomes larger, which results in a smaller value of the nonlinear phase shift ϕ. Therefore we can obtain the weak splitting beam spots. While under the suppression condition, the intensity of the FWM signal $I_{\rm F1}'$ becomes significantly weaker and the spatial splitting will be stronger correspondingly as shown in Fig. 4(b).

The powers of various fields can dramatically affect the enhancement or the suppression of $\boldsymbol{E}_{\rm F1}$. First, we study the switch of by $\boldsymbol{E}_3$ field. Initially, when the power of $\boldsymbol{E}_3$ is small, the singly-dressed system is observed. The signal of $\boldsymbol{E}_{\rm F1}$ is purely enhanced at $\Delta_1 = 57.6$ GHz as shown in Figs. 4(a1)–4(a3) and Figs. 4(b1)–4(b3) because $\boldsymbol{E}_3$ resonates to the dressed state $|G_2-\rangle$ (Fig. 4(d1)) and the enhancement condition $\Delta_1 + \Delta_2 + G_2 = 0$ is matched. Then as the power of $\boldsymbol{E}_3$ increases, the system is doubly-dressed by $\boldsymbol{E}_3$ and $\boldsymbol{E}_2$. The intensity of $\boldsymbol{E}_{\rm F1}$ is first suppressed (under the suppression condition $\Delta_1+\Delta_2 = 0$) and then enhanced (under the enhancement condition $\Delta_1 + \Delta_2 - G_2 = 0$) at $\Delta_1 = 57.6$ GHz (Figs. 4(b4)–(b6)). The corresponding dressed states diagrams are shown in Figs. 4(d2) and 4(d3).

When the power of $\boldsymbol{E}_2$ changes, the switch by $\boldsymbol{E}_2$ is observed too. In such a case, the distance between the two dressed states split by $\boldsymbol{E}_2$ is broadened with the increase of its power. When the power of $\boldsymbol{E}_2$ is little, the distance of $|G_1 - G_2+\rangle$ and $|G_1 - G_2-\rangle$ is relatively small. So $\boldsymbol{E}_3$ gradually resonates to $|G_1 - G_2-\rangle$ (Fig. 4(d4)) and the enhancement condition $\Delta_1 + \Delta_2 + G_2 = 0$ is satisfied. The pure-enhancement is obtained as shown in Figs. 4(c1)–4(c3). Then as the power of $\boldsymbol{E}_2$ becomes larger, the distance between $|G_1-G_2+\rangle$ and $|G_1-G_2-\rangle$ increases, so $\boldsymbol{E}_3$ is first suppressed with the suppression condition $\Delta_1 + \Delta_2 = 0$ satisfied due to the two-photon resonance and then enhanced with the enhancement condition $\Delta_1 + \Delta_2 - G_2 = 0$ matched due to resonance to the dressed state $|G_1 - G_2-\rangle$ (Figs. 4(d5) and 4(d6)). Thus the first suppression and then enhancement is obtained as shown in Figs. 4(c4)–4(c6).

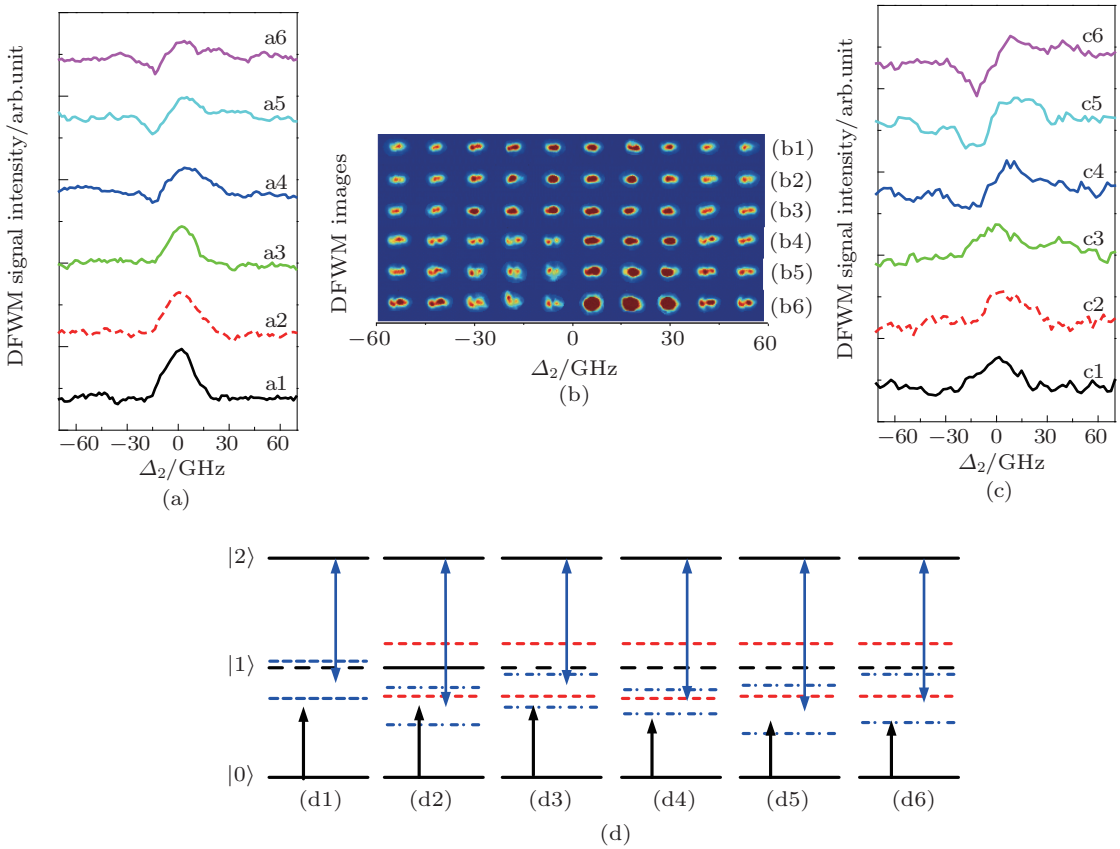


Fig. 4. (colour online) (a) Switch from pure enhancement to first suppression and then enhancement of the DFWM signal $\boldsymbol{E}_{\rm F1}$ when Δ_2 is scanned from −60 GHz to 60 GHz, with different powers of the probe field $\boldsymbol{E}_3$, with the parameters being $P_1 = 12$ μW (power of $\boldsymbol{E}_1$), $P_2 = 25$ μW (power of $\boldsymbol{E}_2$), $\Delta_1 = 57.6$ GHz and P_3 (power of $\boldsymbol{E}_3$)=5.85 (a1), 12 (a2), 12.33 (a3), 16.81 (a4), 20.56 (a5), 23.68 (a6); (b) the corresponding images of $\boldsymbol{E}_{\rm F1}$ in Fig. 4(a). Here panel 4(b) (b1–b6) show that the splittings of $\boldsymbol{E}_{\rm F1}$ signal correspond to the curves in Fig. 4(a) (a1–a6). The condition remains the same as that in Fig. 4(a); (c) the switch from pure enhancement to first suppression and then enhancement of the DFWM signal $\boldsymbol{E}_{\rm F1}$ when Δ_2 is scanned, with different powers of the dressing fields $\boldsymbol{E}_2$, with the parameters being $P_1 = 22$ μW, $P_3 = 10$ μW, $\Delta_1 = 55.4$ GHz and $P_2 = 4.13$ (c1), 7.48 (c2), 10.68 (c3), 13.59 (c4), 16.65 (c5), 19.75 (c6) μW; (d) the dressed state energy diagrams of $\boldsymbol{E}_{\rm F1}$. The first order states are denoted with dashed lines and the second order states are represented with dot-dashed lines.

4. Conclusion

We experimentally investigated the relation between the switch and the spatial splitting of the DFWM signal. By changing the powers of the probe, pump and dressing fields, the switch from pure-enhancement to partial enhancement/suppression can be observed due to the interaction among these fields. Also, the DFWM process evolves from singly-dressed state to doubly-dressed state. The comparisons of the enhancement and the suppression of the DFWM signal between in the two-level atomic system and in the cascade three-level atomic system were made and explained. In addition, we also observed the spatial splittings of the DFWM signal in both x direction and y direction due to the nonlinear cross-Kerr effect and electromagnetically induced grating respectively. The separation distance and number of the splitting beams can be controlled by the intensities and frequencies of the involved laser beams. This work provides detailed mechanisms to optimize the efficiencies of the FWM processes and potential applications in future optical communication and quantum information processing.

References

[1] Agrawal G P 1990 *Phys. Rev. Lett.* **64** 2487

[2] Hickmann J M, Gomes A S L and de Araujo C B 1992 *Phys. Rev. Lett.* **68** 3547

[3] Zhang Y P, Wang Z G, Nie Z Q, Li C B, Chen H X, Lu K Q and Xiao M 2011 *Phys. Rev. Lett.* **106** 093904

[4] Moseley R R, Shepherd S, Fulton D J, Sinclair B D and Dunn M H 1996 *Phys. Rev.* A **53** 408
[5] Harris S E 1997 *Phys. Today* **50** 36S
[6] Yan M, Rickey E G and Zhu Y F 2001 *Phys. Rev.* A **64** 013412
[7] Hemmer P R, Katz D P, Donoghue J, Cronin-Golomb M, Shahriar M S and Kumar P 1995 *Opt. Lett.* **20** 982
[8] Wu Y and Yang X X 2007 *Phys Rev.* A **76** 013832
[9] Wu Y and Yang X X 2004 *Phys Rev.* A **70** 053818
[10] Li C B, Zhang Y P, Nie Z Q, Zheng H B, Shi M Z, Liu D N, Song J P and Lu K Q 2009 *Chin. Phys.* B **18** 5354
[11] Song Y, Dai G X, Fu Y X, Zhao J Y, Wang Z G and Zhang Y P 2011 *Chin. Phys.* B **20** 074206
[12] Nie Z Q, Zheng H B, Li P Z, Yang Y M, Zhang Y P and Xiao M 2008 *Phys. Rev.* A **77** 063829
[13] Zhang Y P, Nie Z Q, Wang Z G, Li C B, Wen F and Xiao M 2010 *Opt. Lett.* **35** 3420